

Theoretical Chromospheres of Late Type Stars

I. Acoustic Energy Generation

A. Renzini¹, C. Cacciari¹, P. Ulmschneider² and F. Schmitz²

¹Osservatorio Astronomico Universitario, CP 596, Bologna, Italy

²Institut für Astrophysik, Universität Würzburg, Am Hubland, D-8700 Würzburg, Federal Republic of Germany

Received January 13, 1977

Summary. For stars in the range $T_{\text{eff}} = 2800$ K to 10000 K and $\log g = -1$ to 6 the acoustic energy flux πF_m generated in the convection zone is computed using the mixing-length theory and the Lighthill theory of sound generation. When convection is efficient and H_2 is not present in the atmosphere, πF_m is roughly proportional to $\alpha^{2.8} g^{-0.7} T_{\text{eff}}^{12}$, α being the ratio of the mixing length to the pressure scale height. At lower T_{eff} , when all hydrogen is in molecular form, one has $\pi F_m \sim g^{-1.2} T_{\text{eff}}^{20}$ and the α -dependence is less pronounced. Finally, the typical period of the acoustic waves is evaluated.

Key words: stellar acoustic fluxes — convection — stellar chromospheres — mass loss

1. Introduction

The recent observational confirmation of the existence of short period (as compared to the local cut-off period) acoustic waves in the sun (Deubner, 1976) places the acoustic heating theory of the chromosphere on a much more solid foundation. This theory goes back to Biermann (1946) and pictures the chromospheric temperature rise as due to the dissipation of shock waves which develop out of acoustic waves that are generated in the convection zone. About ten years ago (Osterbrock, 1961; Kuperus, 1965, 1969; Kopp, 1968) it was almost universally assumed that the chromosphere appears to be heated by acoustic waves with typical periods of five minutes which had been discovered by Leighton and coworkers in 1960 (Leighton, 1960; Leighton et al., 1962). These 5 min oscillations are now known to be generated by nonradial pulsations of the sun (e.g. see Ando and Osaki, 1975; Deubner, 1975, 1976, Ulmschneider, 1976). About five years ago a comparison of empirical chromospheric radiation loss with theoretical dissipation rates of the acoustic shock waves of various mechanical fluxes and periods strongly suggested a short

period nature of the waves (Ulmschneider, 1970, 1974). This was in good agreement with theoretical computations of the spectrum of the acoustic flux produced in the convection zone (Stein, 1968). Stein found a flux maximum at periods of around 30 s which is about one tenth of the local cut-off period. These computations were based on the Lighthill theory of quadrupole sound generation (Lighthill, 1952, 1954; Proudman, 1952; Stein, 1967). However these theoretical results were not considered as definitive especially since such short period waves were not observed. Thus it is not surprising that up to very recently many authors favoured the five minutes oscillation as the mechanism for the chromospheric heating (De Jager, 1975; Praderie and Thomas, 1975). On the other hand the observational discovery of the short period waves in the solar atmosphere (Deubner, 1976), and recent computations showing that short period waves carrying Stein's (1968) flux values are able to predict the location of the solar temperature minimum and at the same time are able to meet the chromospheric energy requirements (Ulmschneider et al., 1976; Kalkofen and Ulmschneider, 1977; Ulmschneider and Kalkofen, 1977; Ulmschneider, 1977), strongly point now in favour of the short period heating theory for the solar chromosphere.

It is thus of great interest to extend these calculations to stars other than the sun in order to compare them with a growing body of empirical models of stellar chromospheres (Ayres et al., 1974; Ayres, 1975; Ayres and Linsky, 1975a, b; Haisch and Linsky, 1976). Furthermore, the knowledge of the temperature structure of the stellar upper atmosphere is crucial in discriminating among rival theories of mass loss in late type giants and supergiants.

It has been suggested that mass loss is due to radiation pressure on molecules (Maciel, 1975) or on grains (e.g. Gehrz and Woolf, 1971; Salpeter, 1974; Lucy, 1976), or on the contrary, that mass loss is driven by the continuous evaporation of the stellar chromosphere/corona like for the solar wind (e.g. Fusi-Pecci and Renzini, 1975a, b, 1976; Renzini, 1976). The determination of stellar chro-

Send offprint requests to: A. Renzini

ospheric temperature minima is then of primary importance since only if such a temperature minimum is low enough grains or molecules can actually form close to the stellar surface. As far as the solar wind-like theory is concerned, the construction of theoretical stellar chromospheric models represents a first step in the direction of eventually describing the whole structure of the stellar chromosphere, corona and wind.

In this paper, which is the first of a series on theoretical stellar chromospheres, we discuss the acoustic energy generation in stars. In Paper II (Ulmschneider et al., 1977) we will present the results of computations concerning the wave propagation in stellar atmospheres, the shock formation and the determination of the temperature minimum. For the chemical composition $X=0.7$, $Y=0.28$ and $Z=0.02$ we have computed the acoustic flux and the period of the acoustic waves for a number of stellar surface gravities and effective temperatures in the range $-1 \leq \log g \leq 6$ and $3.45 \leq \log T_{\text{eff}} \leq 4.00$. The whole set of computations was repeated for three values of the ratio of the mixing length to the pressure scale height, $\alpha = l/H_p = 0.5, 1$ and 1.5 .

2. The Computational Procedure

For the computations we have used the envelope part of a stellar interior program whose main characteristics are described by Castellani and Renzini (1968, 1969) and Castellani et al. (1971a). The Cox and Stewart (1970a, b) opacity tables have been used together with a cubic interpolation procedure (Castellani et al., 1971b). The standard mixing length theory of convection in the form described by Cox and Giuli (1968) was used to derive the convective temperature gradient ∇ and the average convective velocity \bar{v} . This latter quantity is given by

$$\bar{v} = \frac{\alpha}{2} \left(\frac{QP}{2\rho} \right)^{1/2} \left(\frac{\nabla_r - \nabla_{ad}}{9/4 A} \right)^{1/3} \xi^{1/3}, \quad (1)$$

where

$$\xi = \frac{\nabla_r - \nabla}{\nabla_r - \nabla_{ad}} \quad (2)$$

and the notations are the same as in Cox and Giuli. Since \bar{v} depends on the difference of two gradients special care is required in solving the equations of the mixing length theory. Approximate procedures for obtaining ∇ (e.g. Baker and Kippenhahn, 1962) may give unrealistic values of \bar{v} particularly when ∇ is close to ∇_r . For this reason we have used the iterative procedure suggested by Cox and Giuli (1968, p. 314). However, when the quantity B (see Cox and Giuli, 1968, p. 313) is close to unity the iterative procedure does not converge and in these cases a cubic interpolation in the Cox and Giuli (1968, Table 14.2) has been used. Under special circum-

stances Equation (1) gives a supersonic convective velocity which obviously indicates that the mixing length theory is, at least in such cases, inadequate to describe the convective process. Cox and Giuli (1968, p. 324) suggest to limit the convective velocity to the sound velocity v_s , insisting that $\bar{v} = v_s$ when supersonic convective velocities are indicated by Equation (1). However we do not agree with their derivation of the convective gradient since they still used their Equation 14.30b for the convective velocity (setting $\bar{v} = v_s$) which was derived under the assumption that the only force acting on a convective element is the buoyancy force. It is obvious that if \bar{v} has to be limited to subsonic velocities other forces (e.g. drag forces) must be acting on the convective elements. This explains why Cox and Giuli's Equation (14.125) for ∇ gives values which do not match continuously those given by the standard procedure in the adjacent subsonic regions. On the other hand, inserting $\bar{v} = v_s$ in the Cox and Giuli Equations (14.18) and (14.39), which appears more appropriate, one gets

$$\nabla = \frac{(1 + \Gamma)H\nabla_r + D\nabla_{ad}}{(D + H)\Gamma + H} \quad (3)$$

where

$$H = \frac{4ac}{3} \frac{gT^4}{\kappa P} \quad \text{and} \quad D = \frac{1}{2} \rho c_p v_s \alpha T. \quad (4)$$

Equation (3) gives a continuous convective gradient at the edges of the supersonic region, and agrees with the expression given by Iben (1971) in the limit $\nabla' \rightarrow \nabla_{ad}$. Equation (3) then appears physically more reasonable than the corresponding Equation 14.125 of Cox and Giuli, but, of course, we share in all the skepticism of Cox and Giuli (1968, p. 325) about the validity of any version of the mixing length theory and in particular under such extreme physical conditions.

Using the above described input physics, a set of envelope models have been computed. Each model consists of an inward integration, in plane-parallel approximation, down to the bottom of the convective envelope, or more frequently, down to a point where the acoustic energy generation becomes negligible. The total acoustic flux has been computed (Lighthill, 1952, 1954; Proudman, 1952) as

$$\pi F_m = \frac{1}{2} \int 38\rho \frac{\bar{v}^8}{lv_s^5} dr. \quad (5)$$

Equation (5) has been integrated, together with the stellar structure equations, using a 4th order Runge-Kutta procedure wherein the step size was chosen in such a way that the flux changes only by a few percent at each step. In order to test the program we computed, for solar input parameters, and in the non plane parallel approach, the fractional depth of the convection zone $\Delta R/R_\odot$ as a function of the parameter α . These values are compared with those of Baker (1968) in Table 1. The agreement

Table 1 Fractional depth $\Delta R/R_\odot$ and total acoustic flux πF_m as a function of the parameter $\alpha = l/H_p$ for a solar type star. Values in brackets are from Baker (1968)

α	0.5	1.0	1.5	2.0	2.5
$\frac{\Delta R}{R_\odot}$		(0.16)	(0.27)	(0.33)	(0.37)
	0.02	0.14	0.25	0.31	0.34
πF_m (erg/cm ² s)	2.4E6	1.6E7	5.1E7	1.1E8	1.8E8

may be considered satisfactory. Table 1 gives also the corresponding solar acoustic fluxes for each value of α . One finds πF_m proportional to $\alpha^{2.77}$. Allowing for an order of magnitude uncertainty both in observation and theory our solar acoustic fluxes are in agreement with observations (Deubner, 1976) as well as with more refined calculations (Stein, 1968). The chromospheric emission of about $6 \cdot 10^6$ erg/cm² s which may be computed from empirical solar models (Osterbrock, 1961; Athay, 1966; Ulmschneider, 1974; Ayres, 1975) is a lower limit because strong radiation damping of the acoustic waves occurs in the photosphere at $\tau = 0.1$ to 10. Allowing for a factor of 10 decrease of the acoustic flux due to radiation damping (Ulmschneider and Kalkofen, 1977) good agreement is found with our computed total acoustic flux (see also Ulmschneider et al., 1977).

3. The Convective Velocities

The acoustic energy generation depends sensitively on the convective velocity [cf. Eq. (5)]. It is then of primary importance to consider how the convective velocity varies as a function of the model input parameters. Figure 1 shows $(\bar{v}/v_s)_{\max}$, the maximum value of the convective velocity in units of the local sound velocity, as a function of the effective temperature, for various surface gravities and for $\alpha = 1$. The very sharp cut-off of the convective velocity at high effective temperatures is due to the transition from efficient to inefficient convection. In fact when the convection is efficient ∇/∇_r is small and, from Equations (1) and (2) \bar{v} can be large. But, as ∇ approaches ∇_r , the convective velocity drops to zero. Then for each surface gravity the location of the maximum value of $(\bar{v}/v_s)_{\max}$ roughly marks the effective temperature at which the transition between inefficient and efficient convection occurs. When convection is efficient one has approximately

$$\pi F_{\text{conv}} = \rho c_p \bar{v} \Delta T \approx \sigma T_{\text{eff}}^4, \quad (6)$$

where c_p is the specific heat at constant pressure, ΔT is the mean temperature excess of the convective elements relative to their surrounding, and σ is the Stefan-Boltzmann constant. The maximum value of \bar{v} is then expected to occur at small ρ , that is, close to the top of the convection zone, which is actually the case in our models. Following Stein (1966, p. 18) we compute the

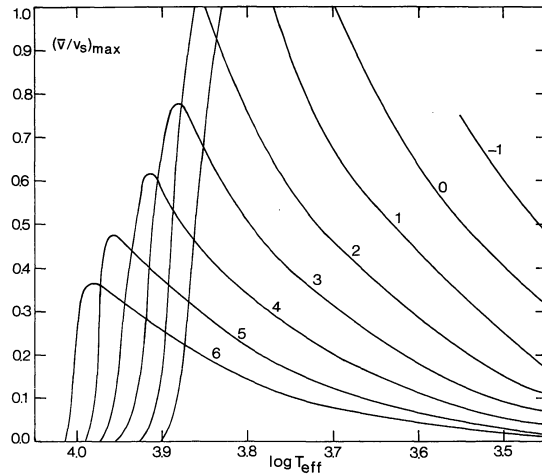


Fig. 1. The maximum value of the ratio of the convective velocity to the sound velocity vs. effective temperature, for $\log g = -1$ to 6 and for $\alpha = 1$

density at the top of the convection zone where $\tau \approx 2/3$ and $T = T_{\text{eff}}$:

$$\rho_{\text{ph}} = \frac{\mu}{R} \left(\frac{2}{3} \frac{a+1}{\kappa_0} \right)^{1/(a+1)} g^{1/(a+1)} T_{\text{eff}}^{-(a+b+1)/(a+1)}. \quad (7)$$

Here μ is the mean molecular weight and R the gas constant. The values of κ_0 , a and b for the H^- opacity are given by Stein (1966, p. 20) to be $\kappa_0 = 6.9E-26$, $a = 0.7$ and $b = 5.3$. From the mixing length theory we find

$$\bar{v} = \left[\frac{g}{T} \left(\frac{dT'}{dr} - \frac{dT}{dr} \right) \right]^{1/2} \frac{l}{2} \quad (8)$$

$$\Delta T = \left(\frac{dT'}{dr} - \frac{dT}{dr} \right) \frac{l}{2},$$

where dT'/dr is the temperature gradient of the convective element. Using

$$l = \alpha H_p = \alpha \frac{RT}{\mu g} \quad (9)$$

we have

$$\Delta T = \bar{v}^2 \frac{2\mu}{\alpha R}. \quad (10)$$

From Equations (6), (7) and (9) we thus find

$$\bar{v} = \left(\frac{\alpha \sigma R}{5\mu} \right)^{1/3} \left[\left(\frac{3}{2} \frac{a+1}{\kappa_0} \right) g T_{\text{eff}}^{-(5a+b+5)} \right]^{-1/(a+3)} \quad (11)$$

with

$$v_s^2 = \gamma \frac{RT}{\mu}. \quad (12)$$

where γ is the ratio of the specific heats, and inserting in Equation (11) the values for κ_0 , a and b one gets

$$\bar{v}/v_s \sim \alpha^{1/3} g^{-0.2} T_{\text{eff}}^{2.2}. \quad (13)$$

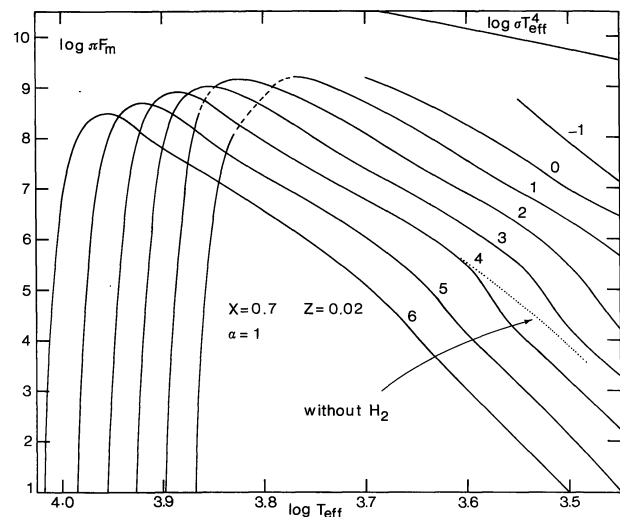


Fig. 2. The acoustic flux πF_m (erg/cm² s) vs. effective temperature, for $\log g = -1$ to 6, $X=0.7$, $Z=0.02$ and $\alpha=1$. The dashed portions of the lines indicate that in the corresponding models supersonic convective velocities occur. The dotted line shows the behaviour of the acoustic flux at low temperatures without taking into account the formation of molecular hydrogen. The straight line in the upper right corner represents the total flux

This agrees well with the $\bar{v}/v_s \sim \alpha^{0.35} g^{-0.21} T_{\text{eff}}^{2.1}$ dependence that we find for the models at low effective temperature, for which the assumption of efficient convection is valid. At a given gravity, relation (13) becomes less and less accurate as the effective temperature increases towards the value at which the maximum in \bar{v}/v_s occurs.

It is worth emphasizing that the dependence of the convective velocity on the mixing length is rather moderate, which is an important point as far as the sound generation is concerned. For $\log g = -1$ and $\log g = 0$ it was impossible to obtain reliable model envelopes for $\log T_{\text{eff}} > \sim 3.55$ and $> \sim 3.70$ respectively. In fact, for such effective temperatures, in the region of density inversion the density is so low and the temperature so high that temperature and density values are encountered for which the Cox-Stewart tables do not provide the opacity. Even if our interpolation procedure formally gives a value for the opacity this value is obviously not reliable and so the whole envelope model.

In conclusion it is worth noting that the mixing length theory is self-consistent only as far as the convective velocity is small compared to the sound velocity. From Figure 1 one sees that at low effective temperatures (typical of red giants and supergiants) \bar{v} is never very large and we may be relatively confident in the reliability of the models. Less reliable are the models at higher effective temperature when \bar{v} approaches v_s .

4. The Acoustic Fluxes

As anticipated in the previous sections, the acoustic flux for each model has been computed using Equation (5).

The region in the convective envelope in which most of the acoustic flux is produced normally coincides with the hydrogen ionization region. In low T_{eff} and high g models the bulk of the acoustic flux is produced in the region of molecular hydrogen dissociation. Figure 2 shows the acoustic flux πF_m as a function of the effective temperature, for $\alpha=1$ and for $\log g = -1$ to 6. Each curve has the same character: the sharp cut-off at high temperatures is obviously due to the cut-off in the convective velocity, while the maximum is clearly associated with the maximum in the convective velocity (cf. Fig. 1). In the region of moderately high temperatures after the maximum we see an approximate $g^{-0.7} T_{\text{eff}}^{1.2}$ behaviour.

In the framework of the analytical approximation described in the previous section, from Equation (5) the acoustic flux can be estimated as

$$\pi F_m \approx \rho_{\text{ph}} \bar{v}^8 / v_s^5, \quad (14)$$

where it has been assumed that the flux is produced within a layer of width $\Delta r \approx l$.

Using Equations (7), (11) and (12) one gets

$$\pi F_m \sim \alpha^{8/3} g^{-5/(3a+3)} T_{\text{eff}}^{(59(a+1)+10b)/(6a+6)} \quad (15)$$

and inserting the values of a and b pertinent to the H^- opacity one obtains a behaviour of the type $\pi F_m \sim \alpha^{8/3} g^{-1} T_{\text{eff}}^{1.5}$. Compared to the crudeness of the approximations, this is in reasonable agreement with the numerical results. At lower effective temperatures, each curve is characterized by a sudden change in slope. According to the numerical models this increase in slope is associated with the appearance of molecular hydrogen in the atmosphere. When hydrogen is completely in molecular form, the slope slightly decreases and remains nearly constant. So, in the low temperature region one has a behaviour of the type $\pi F_m \sim g^{-1.2} T_{\text{eff}}^{2.0}$. If the formation of molecular hydrogen is neglected in the model computation (but still using the same opacity tables) the region of rapidly varying slope disappears (see Fig. 2), which confirms that the “knee” is due to the formation of H_2 . The sudden decrease of the acoustic flux associated with the formation of molecular hydrogen can be understood looking at Equation (11) for the convective velocity. As the H_2 molecules begin to form in the stellar atmosphere, the mean molecular weight increases up to almost a factor of two when all hydrogen is in molecular form. Correspondingly, we have then an increase in the photospheric density. Since, from Equations (11) and (14) one has $\pi F_m \sim \mu_{\text{ph}}^{-5/3}$ an increase in μ_{ph} by a factor of two clearly produces the numerically computed depression in πF_m .

As far as the α -dependence of πF_m is concerned, the numerical results indicate $\pi F_m \sim \alpha^{2.8}$ in good agreement with Equation (15). However in the range of temperatures and gravities in which the H_2 molecule is present in the envelope, the acoustic flux is less sensitive to variations of the mixing length. From Figure 3, which shows πF_m for $\alpha=1.5$, one sees that the “knee” is more pro-

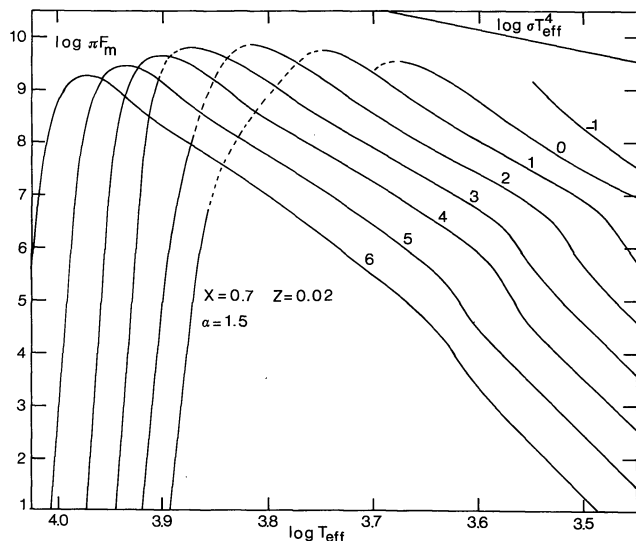


Fig. 3. The same as in Figure 2, for $\alpha = 1.5$

nounced that in the case $\alpha = 1$. This can be easily understood bearing in mind that an increase in α produces a decrease in the temperature gradient and then the H_2 molecules will be dissociated at a deeper layer. Since it is generally supposed that α lies in the range between 0.5 and 1.5 our results indicate that, *due only to the uncertainty in α* , the uncertainty in the absolute value of πF_m is about one order of magnitude. However, the *relative* behaviour of πF_m as a function of g and T_{eff} may be even more interesting than its absolute value, and we can be relatively confident in the trend shown in Figure 2, particularly in the region of efficient convection.

We have also computed a few envelope models using spherical geometry. In this case, besides g and T_{eff} , the stellar mass needs to be specified in order to start the integration. At fixed g and T_{eff} the variation of πF_m with the stellar mass provides a measure of the effect of the deviation from plane geometry. In the range $0.8 - 40 M_{\odot}$ we found no significant variation of πF_m with the mass for $\log g = 6$ and a variation of only 20% for $\log g = -1$. This means that the assumption of plane geometry is well justified as far as the computation of the acoustic flux is concerned.

Figure 4 shows the lines of equal acoustic flux in the $\log g - \log T_{\text{eff}}$ plane for $\alpha = 1$. The locations of the Zero Age Main Sequence (ZAMS), of the Population II giant branch and of Population I supergiants are indicated. For main sequence stars, maximum acoustic fluxes are expected in the range of effective temperatures $\log T_{\text{eff}} = 3.95$ to 3.80 , i.e. for late A to early F type stars. For Population II giants the acoustic flux moderately increases along the giant branch. Among Population I

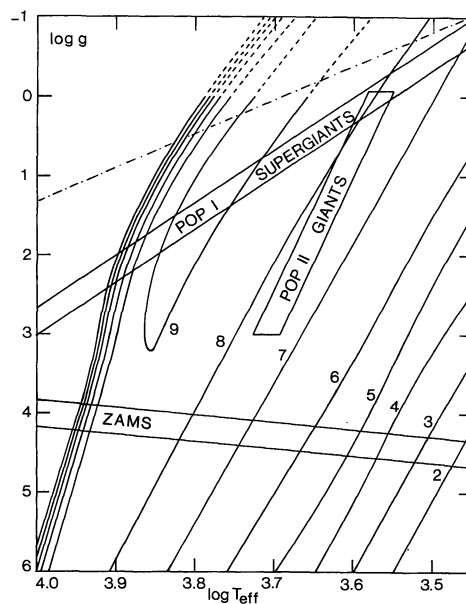


Fig. 4. The lines of equal acoustic flux $\log \pi F_m$ ($\text{erg/cm}^2 \text{ s}$) as a function of g and T_{eff} , for $\alpha = 1$. The location of the Zero Age Main Sequence (ZAMS), of the Population II giant branch and of Population I supergiants are indicated. The dotted-dashed line is the approximate path of a $40 M_{\odot}$ star

supergiants the F type stars should have maximum acoustic fluxes. Since, apart from the white dwarfs, real stars populate the region between the ZAMS and the Population I supergiant strip, the region of low $g - \text{high } T_{\text{eff}}$ (for which it was impossible to construct reliable model envelopes) is never crossed by evolving stars. The topology of the iso-acoustic lines in Figure 4 is preserved as α varies.

A qualitative agreement is found with previous computations (Nariai, 1969; De Loore, 1970). However, in the previous investigations either not the whole range of effective temperatures was covered (Nariai) or not the same input physics was used for the whole range of effective temperatures (De Loore). In De Loore's work the opacity tables taken for the regions at high T_{eff} are different from those used at small T_{eff} causing an unphysical discontinuity between $T_{\text{eff}} = 4000$ K and 4750 K. Kippenhahn (1973) used the De Loore results to construct iso-acoustic lines in the range $\log T_{\text{eff}} = 3.4 - 4.0$. The differences in topology with respect to our Figure 4 are entirely due to the mentioned discontinuity in the input physics at $T_{\text{eff}} = 4000$ K. The two-lobe structure of the De Loore-Kippenhahn iso-acoustic lines is thus spurious. A two-lobe structure, however, is found if very large values of α are used or if the mixing length is taken proportional to the density scale height (cf. Castellani et al., 1971) but both these assumptions appear to be unrealistic.

Aside from these qualitative differences, the acoustic fluxes computed by De Loore are in general roughly one order of magnitude larger than those computed by us. This difference arises primarily from a different numerical

factor used in the expression for the convective velocity [compare De Loore's Eq. (4) with Cox and Giuli's Eq. (14.28b)]. This disagreement gives an idea of what happens when one uses slightly different versions of the mixing length theory.

Finally, the upper straight line in Figure 2 gives the total flux T_{eff}^4 . An inspection of Figure 2 reveals that the maximum acoustic flux is at most a few percent of the total energy flux.

5. The Period of the Acoustic Waves

In a more detailed calculation than that described in Section 2, Stein (1968) has computed in the solar case the monochromatic flux of acoustic waves as a function of the wave period P . Stein (1970) has also computed the acoustic spectra for different kinds of stars. Stein and Leibacher (1975) have found that the period P_{max} at which the monochromatic acoustic flux has its maximum is about a factor of ten smaller than the acoustic cut-off period P_a at the point of maximum flux generation:

$$P_{\text{max}} \approx \frac{1}{10} P_a = \frac{1}{10} 4\pi v_s / \gamma g. \quad (16)$$

For each envelope model we have computed P_{max} using for v_s and γ their values at the level of maximum flux generation. It is seen that P_{max} depends mainly on gravity and only very slightly on T_{eff} . This is due to the fact that the temperature enters in Equation (19) only as a square root. P_{max} is also nearly independent of α . A good fit to our numerical results is:

$$\log P_{\text{max}} = 5.8 - \log g. \quad (17)$$

Since the boundary temperature is at most a factor of two smaller than the temperature corresponding to v_s in Equation (19), we see that the period P_{max} is still much smaller than the cut-off period of the photospheric layers. This indicates that the acoustic flux propagates unimpeded into the outermost layers (apart from the radiative damping effects).

6. Discussion

It is universally known that the mixing length theory provides only a very crude representation of the physical structure of convective envelopes. Our models then suffer from this obvious source of uncertainty. A second critical point, as far as the evaluation of the acoustic flux is concerned, is represented by our ignorance of the actual spectrum of the convective velocity at each depth in the star. In this respect Stein (1968) has shown that the acoustic flux depends sensitively on the assumed spectrum. In practice we have assumed a delta function at $v = \bar{v}$ for the velocity spectrum, which is a very rough approximation. The third source of uncertainty is represented by the use of the Lighthill theory of sound generation, whose applicability to astrophysical situations still waits to be proven. These uncertainties in the computations of

stellar acoustic fluxes are widely known (see for instance Jordan, 1973; Athay, 1975; Stein and Leibacher, 1975) and we concur with the general scepticism. On the other hand a justification for our simple approach is that, at the moment, it is practically impossible to do better. Ultimately, only a comparison of our theoretical predictions with the observations of stellar chromospheres can decide whether our computations have something in common with reality.

A comparison with observations will be made in the next paper, in which we compute theoretical chromospheric temperature minima.

References

- Ando, H., Osaki, Y.: 1975, *Publ. Astron. Soc. Japan* **27**, 581
 Athay, R. G.: 1966, *Astrophys. J.* **146**, 223
 Athay, R. G.: 1975, *The Solar Chromosphere and Corona*, Reidel Publ. Comp. Dordrecht
 Ayres, T. R.: 1975, Ph. D. Thesis, University of Colorado, Boulder
 Ayres, T. R., Linsky, J. L., Shine, R. A.: 1974, *Astrophys. J.* **192**, 93
 Ayres, T. R., Linsky, J. L.: 1975a, *Astrophys. J.* **200**, 660
 Ayres, T. R., Linsky, J. L.: 1975b, *Astrophys. J.* **201**, 212
 Baker, N.: 1968, see Cox and Giuli (1968), p. 612
 Baker, N., Kippenhahn, R.: 1972, *Z. Astrophys.* **54**, 114
 Biermann, L.: 1946, *Naturwiss.* **33**, 118
 Castellani, V., Giannone, P., Renzini, A.: 1971a, *Mem. Soc. Astron. Ital.* **42**, 221
 Castellani, V., Puppi, L., Renzini, A.: 1971b, *Astrophys. Space Sci.* **10**, 136
 Castellani, V., Renzini, A.: 1968, *Astrophys. Space Sci.* **2**, 310
 Castellani, V., Renzini, A.: 1969, *Astrophys. Space Sci.* **3**, 283
 Cox, J. P., Giuli, R. T.: 1968, *Principles of Stellar Structure*, Gordon & Breach, New York
 Cox, A. N., Stewart, J. N.: 1970a, *Astrophys. J. Suppl.* **19**, 243
 Cox, A. N., Stewart, J. N.: 1970b, *Astrophys. J. Suppl.* **19**, 261
 Deubner, F. L.: 1975, *Astron. Astrophys.* **44**, 371
 Deubner, F. L.: 1976, *Astron. Astrophys.* **51**, 189
 Fusi-Pecci, F., Renzini, A.: 1975a, *Astron. Astrophys.* **39**, 413
 Fusi-Pecci, F., Renzini, A.: 1975b, Proceedings of the 19th Int. Coll. on Problems in Stellar Hydrodynamics, Liège, ed. M. Gabriel, *Mem. Soc. Roy. Sci. Liège*, 6th Series, **8**, 383
 Fusi-Pecci, F., Renzini, A.: 1976, *Astron. Astrophys.* **46**, 447
 Gehrz, R. D., Woolf, N. J.: 1971, *Astrophys. J.* **165**, 285
 Haisch, B. M., Linsky, J. L.: 1976, *Astrophys. J. Letters* **205**, L39
 Iben, I.: 1971, *Astrophys. J.* **166**, 131
 De Jager, C.: 1975, *Mitt. Astron. Gesell.* **36**, 15
 Jordan, S. D.: 1973, Proceedings of the IAU Colloquium No. 19 on "Stellar Chromospheres", p. 181, Eds. S. D. Jordan and E. H. Avrett
 Kalkofen, W., Ulmschneider, P.: 1977, *Astron. Astrophys.* **57**, 193
 Kippenhahn, R.: 1973, Proceedings of the IAU Colloquium No. 19 on "Stellar Chromospheres", p. 265, Eds. S. D. Jordan and E. H. Avrett
 Kondo, Y., Morgan, T. H., Modisette, J. L.: 1976, *Astrophys. J.* **209**, 489
 Kopp, R.: 1968, Ph. D. Thesis, Harvard University, Cambridge, Mass.
 Kuperus, M.: 1965, *Rech. Astron. Obs. Utrecht* **17**, 1
 Kuperus, M.: 1969, *Space Sci. Rev.* **9**, 713
 Leighton, R. B.: 1960, IAU Symposium No. 12, "Cosmical Gas Dynamics", ed. R. Thomas
 Leighton, R. B., Noyes, R. W., Simon, G. W.: 1962, *Astrophys. J.* **135**, 474
 Lighthill, M. J.: 1952, *Proc. Roy. Soc. London* **A211**, 564
 Lighthill, M. J.: 1954, *Proc. Roy. Soc. London* **A222**, 1
 De Loore, C.: 1970, *Astrophys. Space Sci.* **6**, 60
 Lucy, L. B.: 1976, *Astrophys. J.* **205**, 482

- Maciel, W. J.: 1975, *Astron. Astrophys.* **48**, 27
Nariai, K.: 1969, *Astrophys. Space Sci.* **3**, 150
Osterbrock, D.: 1961, *Astrophys. J.* **134**, 347
Praderie, F.: 1973, Proceedings of the IAU *Colloquium* No. 19 on "Stellar Chromospheres", p. 79, Eds. S. D. Jordan and E. H. Avrett
Praderie, F., Thomas, R.: 1975 (private communication)
Proudman, I.: 1952, *Proc. Roy. Soc. London A* **214**, 119
Renzini, A.: 1976, The Galaxy and the Local Group, Roy. Greenwich Obs. Bull. **182**, eds. R. J. Dickens and J. E. Perry
Salpeter, E. E.: 1974, *Astrophys. J.* **193**, 585
Stein, R. F.: 1966, *Astron. J.* **71**, 181
Stein, R. F.: 1967, *Solar Phys.* **2**, 385
Stein, R. F.: 1968, *Astrophys. J.* **154**, 297
Stein, R. F.: 1970 (private communication)
Stein, R. F., Leibacher, J.: 1975, *Ann. Rev. Astron. Astrophys.* **12**, 407
Ulmschneider, P.: 1970, *Solar Phys.* **12**, 403
Ulmschneider, P.: 1974, *Solar Phys.* **39**, 327
Ulmschneider, P.: 1976, *Solar Phys.* **49**, 249
Ulmschneider, P.: 1977, *Mem. Soc. Astron. Ital.* (to be published)
Ulmschneider, P., Kalkofen, W., Nowak, T., Bohn, M. U.: 1976, *Astron. Astrophys.* (in press)
Ulmschneider, P., Kalkofen, W.: 1977, *Astron. Astrophys.* (in press)
Ulmschneider, P., Schmitz, F., Renzini, A., Cacciari, C., Kalkofen, W., Kurucz, R.: 1977 (in preparation) (Paper II)